# Preparation and Characterization of Polypseudorotaxanes Based on Block-Selected Inclusion Complexation between Poly(propylene oxide)-Poly(ethylene oxide)-Poly(propylene oxide) Triblock Copolymers and α-Cyclodextrin

Jun Li,*,†,‡ Xiping Ni,† Zhihan Zhou,† and Kam W. Leong†,§

*Contribution from the Institute of Materials Research and Engineering (IMRE), 3 Research Link, Singapore 117602, Republic of Singapore; Division of Bioengineering, Faculty of Engineering, National University of Singapore, Singapore 117576, Republic of Singapore; and Department of Biomedical Engineering, Johns Hopkins University, Baltimore, Maryland 21205, USA.*

Received April 22, 2002; E-mail: jun-li@imre.a-star.edu.sg

***Abstract:*** A series of new polypseudorotaxanes were synthesized in high yields when the middle poly-(ethylene oxide) (PEO) block of poly(propylene oxide)-poly(ethylene oxide)-poly(propylene oxide) (PPO−PEO−PPO) triblock copolymers was selectively recognized and included by α-cyclodextrin (α-CD) to form crystalline inclusion complexes (ICs), although the middle PEO block was flanked by two thicker PPO blocks, and a PPO chain had been previously thought to be impenetrable to α-CD. X-ray diffraction studies demonstrated that the IC domains of the polypseudorotaxanes assumed a channel-type structure similar to the necklace-like ICs formed by α-CD and PEO homopolymers. Solid-state CP/MAS $^{13}$C NMR studies showed that the α-CD molecules in the polypseudorotaxanes adopted a symmetrical conformation due to the formation of ICs. The compositions and stoichiometry of the polypseudorotaxanes were studied using $^1$H NMR, and a 2:1 (ethylene oxide unit to α-CD) stoichiometry was found for all polypseudorotaxanes although the PPO−PEO−PPO triblock copolymers had different compositions and block lengths, suggesting that only the PEO block was closely included by α-CD molecules, whereas the PPO blocks were uncovered. The hypothesis was further supported by the differential scanning calorimetry (DSC) studies of the polypseudorotaxanes. The glass transitions of the PPO blocks in the polypseudorotaxanes were clearly observed because they were uncovered by α-CD and remained amorphous, whereas the glass-transition temperatures increased, because the molecular motion of the PPO blocks was restricted by the hard crystalline phases of the IC domains formed by α-CD and the PEO blocks. The thermogravimetric analysis (TGA) revealed that the polypseudorotaxanes had better thermal stability than their free components due to the inclusion complexation. Finally, the kinetics of the threading process of α-CD onto the copolymers was also studied. The findings reported in this article suggested interesting possibilities in designing other cyclodextrin ICs and polypseudorotaxanes with block structures.

## Introduction

Inclusion complexes (ICs), particularly the ones leading to supramolecular self-assemblies, continue to be a fascinating topic in modern organic chemistry as they serve as models for understanding molecular recognition and as precursors for designing novel nanomaterials for electronics and biological applications. Polyrotaxane, formed by multiple macrocycles threading over a polymer chain, is such an example.[1−4]

Cyclodextrins (CDs) are a series of cyclic oligosaccharides composed of 6, 7, or 8 D(+)-glucose units linked by α-1,4-linkages, and named α-, β-, or γ-CD, respectively. The geometry of CDs gives a hydrophobic cavity having a depth of ca. 7.0 Å, and an internal diameter of ca. 4.5, 7.0, and 8.5 Å for α-, β-, and γ-CD, respectively.[5] Various molecules can be fitted into the cavity of CDs to form ICs, which have been extensively studied as models for understanding the mechanism of molecular recognition.[5,6]

(1) (a) Gibson, H. W.; Marand, H. *Adv. Mater.* **1993**, *5*, 11−21. (b) Gibson, H. W.; Bheda, M. C.; Engen, P. T. *Prog. Polym. Sci.* **1994**, *19*, 843−945. (c) Vogtle, F.; Dunnwald, T.; Schmidt, T. *Acc. Chem. Res.* **1996**, *29*, 451−460. (d) Fyfe, M. C. T.; Stoddart, J. F. *Acc. Chem. Res.* **1997**, *30*, 393−401. (e) Raymo, F. M.; Stoddart, J. F. *Chem. Rev.* **1999**, *99*, 1643−1663. (f) Sauvage, J.-P.; Dietrich-Buchecker, C. *Molecular Catenanes, Rotaxanes and Knots*, VCH: Weinheim, 1999. (g) Semlyen, J. A. *Cyclic Polymers*, Kluwer Academic Publisher: Boston, 2000.
(2) (a) Amabilino, D. B.; Ashton, P. R.; Balzani, V.; Brown, C. L.; Credi, A.; Frechet, J. M. J.; Leon, J. W.; Raymo, F. M.; Spencer, N.; Stoddart, J. F.; Venturi, M. *J. Am. Chem. Soc.* **1996**, *118*, 12 012−12 020. (b) Ashton, P. R.; Ballardini, R.; Balzani, V.; Fyfe, M. C. T.; Gandolfi, M. T.; Martinez-Diaz, M. V.; Morosini, M.; Schiavo, C.; Shibata, K.; Stoddart, J. F.; White, A. J. P.; Williams, D. J. *Chem. Eur. J.* **1998**, *4*, 2332−2341. (c) Wong, E. W.; Collier, C. P.; Behloradsky, M.; Raymo, F. M.; Stoddart, J. F.; Heath, J. R.. *Am. Chem. Soc.* **2000**, *122*, 5831−5840. (d) Chiu, S.-H.; Stoddart, J. F. *J. Am. Chem. Soc.* **2002**, *124*, 4174−4175.
(3) (a) Gong, C. G.; Gibson, H. W. *Macromolecules* **1996**, *29*, 7029−7033. (b) Gong, C. G.; Balanda, P. B.; Gibson, H. W. *Macromolecules* **1998**, *31*, 5278−5289. (c) Mason, P. E.; Bryant, W. S.; Gibson, H. W. *Macromolecules* **1999**, *32*, 1559−1569. (d) Gibson, H. W.; Bryant, W. S.; Lee, S. H. *J. Polym. Sci., Polym. Chem.* **2001**, *39*, 1978−1993.

† Institute of Materials Research and Engineering.
‡ National University of Singapore.
§ Johns Hopkins University.

**Chart 1.** Structure of the PPO−PEO−PPO Triblock Copolymers.
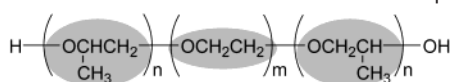


Recently, polypseudorotaxanes, or ICs with necklace-like supramolecular structures formed by cyclodextrins and polymers have attracted special interest.[7−13] The size correlation between the cross-sectional area of the polymer chains and the cavities of CDs plays an important role in the IC formation. Poly-(ethylene oxide) (PEO) and oligoethylene of various molecular weights form ICs with $\alpha$-CD to give crystalline polypseudo-rotaxanes in high yields, but not with $\beta$-CD and $\gamma$-CD.[8] Conversely, poly(propylene oxide) (PPO) can form ICs with $\beta$-CD and $\gamma$-CD in high yields, but not with $\alpha$-CD.[9] The assumption is that the PPO chain is too large to penetrate the inner cavity of $\alpha$-CD. There have been also studies on IC formation of CDs and Pluronic PEO−PPO−PEO triblock copolymers, where thinner PEO blocks flank a middle PPO block. $\beta$-CD would selectively thread the middle PPO block to form a polypseudorotaxane,[10] whereas $\alpha$-CD selectively includes the flanking PEO blocks.[11] Recently, we reported the formation of polypseudorotaxanes between poly[(ethylene oxide)-*ran*-(propylene oxide)] and $\alpha$-CD, and demonstrated that $\alpha$-CD can pass over a PO unit randomly placed in the PEO chain, forming ICs with EO units.[12]

Here, we have unexpectedly found that PPO−PEO−PPO triblock copolymers (known as Pluronic-R or "reverse" Pluronic), where two thicker PPO blocks flank a middle PEO block (Chart 1), can form ICs with $\alpha$-CD to give polypseudorotaxanes in high yields. Although there are two thicker PPO blocks flanking the middle PEO block, it is interesting that the copolymer still can penetrate the smallest cavity of $\alpha$-CD to form polypseudorotaxanes. In this article, we report the preparation and characterization of the $\alpha$-CD-PPO−PEO−PPO poly-pseudorotaxanes, and the studies of the threading and sliding kinetics of $\alpha$-CD onto the copolymer chains. Our results have shown that $\alpha$-CD selectively forms ICs with the middle PEO

block stoichiometrically, and the polypseudorotaxanes contain the crystalline IC domains and the amorphous domains of uncomplexed PPO blocks. It is thought that the enthalpic driving force of complexing $\alpha$-CD with the PEO block can overcome the energy barrier of sliding $\alpha$-CD over the relatively bulky PPO blocks.

## Experimental Section

**Materials**. Three samples of Pluronic-R PPO−PEO−PPO triblock copolymers with different molecular weights and block lengths were purchased from Aldrich. According to the manufacturer, the PPO−PEO−PPO triblock copolymers were synthesized following the procedure shown in Scheme 1, which ensures the PPO blocks are located at the two ends of the copolymers. In this study, we actually determined the molecular characteristics of the three triblock copolymer samples and studied their chain architecture using GPC,^{1}H NMR,^{13}C NMR, and elemental analysis. PEO ($M_n$ 1000) and PPO ($M_n$ 1000) homopolymers were also supplied by Aldrich. $\alpha$-, $\beta$-, and $\gamma$-CDs were obtained from Tokyo Kasei Inc. DMSO-$d_6$ and CDCl$_3$ used as solvents in the NMR measurements were obtained from Aldrich.

**Measurements**. The ^{1}H NMR spectra were recorded on a Bruker AV-400 NMR spectrometer at 400 MHz at room temperature. The ^{1}H NMR measurements were carried out with an acquisition time of 3.2 s, a pulse repetition time of 2.0 s, a 30° pulse width, 5208-Hz spectral width, and 32 K data points. Chemical shifts were referred to the solvent peaks ($\delta = 7.30$ and 2.50 ppm for CDCl$_3$ and DMSO-$d_6$, respectively). The ^{13}C NMR spectra were recorded on a Bruker AV-400 NMR spectrometer at 100 MHz at room temperature. The ^{13}C NMR measurements were carried out using composite pulse decoupling with an acquisition time of 0.82 s, a pulse repetition time of 5.0 s, a 30° pulse width, 20 080-Hz spectral width, and 32 K data points. Chemical shifts were referred to the solvent peaks ($\delta = 77.16$ ppm for CDCl$_3$). The solid-state ^{13}C CP/MAS NMR spectra were measured on a Bruker AV-400 NMR spectrometer at 100 MHz with a sample spinning rate of 5000 Hz at room temperature. CP spectra were acquired with a 4-ms proton 90° pulse, a 1-ms contact time, and a 5-s repetition time. Chemical shifts were referred to external standard adamantane.

Gel permeation chromatography (GPC) analysis was carried out with a Shimadzu SCL-10A and LC-8A system equipped with two Phenogel 5$\mu$ 50 and 1000 Å columns (size: 300 × 4.6 mm) in series and a refractive detector. THF was used as eluent at a flow rate of 0.30 mL/min at 40 °C. Monodispersed poly(ethylene glycol) standards were used to obtain a calibration curve.

Wide-angle X-ray diffraction (XRD) measurements were carried out using a Simens D5005 Diffractometer using Ni-filtered Cu K$_\alpha$ (1.542 Å) radiation (40 kV, 40 mA). Powder samples were mounted on a sample holder and scanned from 5° to 35° in $2\theta$ at a speed of 0.6° per minute.

Differential scanning calorimetry (DSC) measurements were performed under nitrogen flow of 30 mL/min on a TA Instruments 2920 differential scanning calorimeter equipped with a cooling accessory and calibrated using indium. The following protocol was used for each sample: heating from room temperature to 250 °C at 20 °C/min, holding at 250 °C for 20 min, then quenching from 250 °C to −140 °C using liquid

(4) (a) Schmieder, R.; Hubner, G.; Seel, C.; Vogtle, F. *Angew. Chem., Int. Ed. Engl.* **1999**, *38*, 3528−3530. (b) Safarowsky, O.; Vogel, E.; Vogtle, F. *Eur. J. Org. Chem.* **2000**, 499−505.
(5) Bender, M. L.; Komiyama, M. *Cyclodextrin Chemistry*, Springer-Verlag: Berlin, 1978. (b) Szejtli, J. *Cyclodextrins and Their Inclusion Complexes*, Akademiai Kiado: Budapest, 1982.
(6) (a) Szejtli, J. *Chem. Rev.* **1998**, *98*, 1743−1754. (b) Lipkowitz, K. B. *Chem. Rev.* **1998**, *98*, 1829−1874.
(7) (a) Wenz, G. *Angew. Chem., Int. Ed.* **1994**, *33*, 803−822. (b) Nepogodiev, S. A.; Stoddart, J. F. *Chem. Rev.* **1998**, *98*, 1959−1976.
(8) (a) Harada, A.; Li, J.; Kamachi, M. *Nature* **1992**, *356*, 325−327. (b) Harada, A.; Li, J.; Kamachi, M. *Macromolecules* **1993**, *26*, 5698−5703. (c) Li, J.; Harada, A.; Kamachi, M. *Bull. Chem. Soc. Jpn.* **1994**, *67*, 2808−2818. (d) Li, J.; Harada, A.; Kamachi, M. *Polym. J.* **1994**, *26*, 1019−1026.
(9) (a) Harada, A.; Okada, M.; Li, J.; Kamachi, M. *Macromolecules* **1995**, *28*, 8406−8411. (b) Pozuelo, J.; Mendicuti, F.; Mattice, W. L. *Polym. J.* **1998**, *30*, 479−484. (c) Nostro, P. L.; Lopes, J. R.; Cardelli, C. *Langmuir* **2001**, *17*, 4610−4615. (d) Lo Nostro, P.; Lopes, J. R.; Ninham, B. W.; Baglioni, P. J. *Phys. Chem. B* **2002**, *106*, 2166−2174.
(10) Fujita, H.; Ooya, T.; Yui, N. *Macromolecules* **1999**, *32*, 2534−2541.
(11) Li, J.; Li, X.; Zhou, Z.; Ni, X.; Leong, K. W. *Macromolecules* **2001**, *34*, 7236−7237.
(12) Li, J.; Li, X.; Toh, K. C.; Ni, X.; Zhou, Z.; Leong, K. W. *Macromolecules* **2001**, *34*, 8829−8831.
(13) (a) Wenz, G.; Keller, B. *Angew. Chem., Int. Ed. Engl.* **1992**, *31*, 197−199. (b) Herrmann, W.; Keller, B.; Wenz, G. *Macromolecules* **1997**, *30*, 4966−4972. (c) Born, M.; Ritter, H. *Macromol. Rapid Commun.* **1996**, *17*, 197−202. (d) Rusa, C. C.; Luca, C.; Tonelli, A. E. *Macromolecules* **2001**, *34*, 1318−1322. (e) Rusa, C. C.; Tonelli, A. E. *Macromolecules* **2001**, *34*, 5321−5324. (f) Huh, K. M.; Ooya, T.; Sasaki, S.; Yui, N. *Macromolecules* **2001**, 34, 2402−2404. (g) Jiao, H.; Goh, S. H.; Valiyaveettil, S. *Macromolecules* **2002**, *35*, 1980−1983. (h) Li, J.; Uzawa, J.; Doi, Y. *Bull. Chem. Soc. Jpn.* **1998**, *71*, 1953−1957. (i) Li, J.; and Toh, K. C. *J. Chem. Soc., Perkin Trans. 2* **2002**, 35−40.

**Scheme 1.** Synthesis of the PPO-PEO-PPO triblock copolymers.
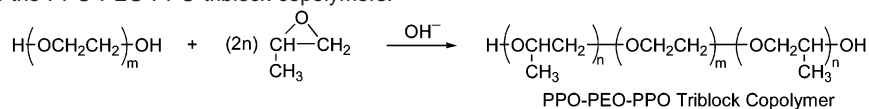


Reaction conditions:
Catalyst, KOH; under $N_2$ atomsphere.
Controlled at 120 °C by adjusting monomer feeding rate.

nitrogen, and finally reheating from −140 °C to 200 °C at 20 °C/min. Data were collected during the second heating run. Transition temperatures were taken as the midpoint of the heat capacity change. Thermogravimetric analyses (TGA) were made using a TA Instrument SDT 2960. Samples were heated at 20 °C min$^{-1}$ from room temperature to 800 °C in a dynamic nitrogen atmosphere at a flow rate of 70 mL/min.

UV−vis spectra were recorded with a Shimadzu UV-2501PC spectrophotometer with a cell temperature controlling unit connected with a thermostated water bath (±0.1 °C). For the threading kinetics studies, 0.3 mL of copolymer aqueous solution (5.0 wt %) and 2.0 mL of α-CD aqueous solution (0.145 g/mL) were mixed in the cuvette (cell length 1.0 cm) at 20 °C, and the absorption measurement (at $\lambda = 600$ nm) was started immediately. The reference sample was pure water.

**Preparation of Polypseudorotaxanes**. The α-CD-PPO− PEO−PPO polypseudorotaxanes were prepared as follows. Bulk PPO−PEO−PPO triblock copolymers (75.0 mg) were added into an excess of α-CD aqueous solution (4.57 mL, 0.145 g/mL) in a test tube at room temperature. The dissolution of the copolymer could be facilitated by immersing the tubes in an ultrasonic waterbath or vortexing.[14] The solutions gradually became turbid, eventually producing polypseudorotaxanes during the formation of ICs as precipitates. The polypseudorotaxanes were isolated by filtration or centrifugation, washed with a limited amount of water, and dried under vacuum. The yield was calculated based on the amount of copolymers used.

**α-CD-PO$_8$EO$_{23}$PO$_8$ Polypseudorotaxane.** Yield, 390 mg, 73%. $^1$H NMR (400 MHz, DMSO-$d_6$, 22 °C): δ 5.51 (s, 68H, O(2)H of CD), 5.43 (s, 68H, O(3)H of CD), 4.80 (d, 68H, H(1) of CD), 4.48 (t, 68H, O(6)H of CD), 3.77 (t, 68H, H(3) of CD), 3.64 (m, 136H, H(6) of CD), 3.58 (m, 68H, H(5) of CD), 3.51 (s, 92H, H of PEO block), 3.25−3.47 (br, m, 185H, H of PPO backbone, H(2) and H(4) of CD), 1.04 (m, 48H, −CH$_3$ of PPO block). Anal. Calcd for C$_{94}$H$_{190}$O$_{40}$·12C$_{36}$H$_{60}$O$_{30}$·24H$_2$O: C, 44.91; H, 6.52. Found: C, 44.45; H, 6.89.

**α-CD-PO$_{15}$EO$_{24}$PO$_{15}$ Polypseudorotaxane.** Yield, 331 mg, 83%. $^1$H NMR (400 MHz, DMSO-$d_6$, 22 °C): δ 5.51 (s, 68H, O(2)H of CD), 5.43 (s, 68H, O(3)H of CD), 4.80 (d, 68H, H(1) of CD), 4.47 (t, 68H, O(6)H of CD), 3.77 (t, 68H, H(3) of CD), 3.64 (m, 136H, H(6) of CD), 3.58 (m, 68H, H(5) of CD), 3.51 (s, 96H, H of PEO block), 3.25−3.47 (br, m, 227H, H of PPO backbone, H(2) and H(4) of CD), 1.04 (m, 90H, −CH$_3$ of PPO block). Anal. Calcd for C$_{138}$H$_{278}$O$_{55}$·12C$_{36}$H$_{60}$O$_{30}$·24H$_2$O: C, 45.87; H, 6.74. Found: C, 45.43; H, 7.21.

**α-CD-PO$_{25}$EO$_{12}$PO$_{25}$ Polypseudorotaxane.** Yield, 146 mg, 71%. $^1$H NMR (400 MHz, DMSO-$d_6$, 22 °C): δ 5.51 (s, 34H, O(2)H of CD), 5.43 (s, 34H, O(3)H of CD), 4.80 (d, 34H, H(1) of CD), 4.47 (t, 34H, O(6)H of CD), 3.77 (t, 34H, H(3) of CD), 3.64 (m, 67H, H(6) of CD), 3.58 (m, 34H, H(5) of CD), 3.50 (s, 48H, H of PEO block), 3.25−3.48 (br, m, 217H, H of PPO

**Table 1.** Molecular Characteristics of the PPO−PEO−PPO Triblock Copolymers Used in This Study

| copolymer[a] | composition[b] | $M_n$[c] | $M_w/M_n$[c] | PPO content[d] (wt %) | anal. calcd[e] C (%) | anal. calcd[e] H (%) | found[f] C (%) | found[f] H (%) |
|---|---|---|---|---|---|---|---|---|
| 1 | PO$_8$EO$_{23}$PO$_8$ | 1990 | 1.04 | 47 | 57.06 | 9.78 | 56.94 | 10.18 |
| 2 | PO$_{15}$EO$_{24}$PO$_{15}$ | 2740 | 1.03 | 60 | 58.45 | 9.95 | 58.04 | 10.14 |
| 3 | PO$_{25}$EO$_{12}$PO$_{25}$ | 3450 | 1.03 | 85 | 60.25 | 10.23 | 60.21 | 10.51 |

[a] The copolymers are denoted PO$_n$EO$_m$PO$_n$ where n and m are average block lengths in repeat units. [b] Determined by combination of $^1$H NMR and GPC results. [c] Determined by GPC. [d] Determined by $^1$H NMR. [e] Elemental analysis calculated for Copolymer 1, C$_{94}$H$_{190}$O$_{40}$·(H$_2$O)$_1$; Copolymer 2, C$_{138}$H$_{278}$O$_{55}$·(H$_2$O)$_1$; and Copolymer 3, C$_{174}$H$_{350}$O$_{63}$·(H$_2$O)$_1$. [f] Elemental analysis found.

backbone, H(2) and H(4) of CD), 1.04 (m, 150H, −CH$_3$ of PPO block). Anal. Calcd for C$_{174}$H$_{350}$O$_{63}$·6C$_{36}$H$_{60}$O$_{30}$·12H$_2$O: C, 49.29; H, 7.53. Found: C, 48.86; H 8.02.

## Results and Discussion

The molecular characteristics of the PPO−PEO−PPO triblock copolymers used in this study are presented in Table 1. The PPO−PEO−PPO triblock copolymers are known as Pluronic-R or "reverse" Pluronic, which were well studied previously,[15] with respect to the effect of the chain architecture. Our GPC data showed that all triblock copolymers presented a single unimodal peak in their GPC chromotograms. The copolymers were found to be nearly monodispersed, with a polydispersity ranging from 1.03 to 1.04. The GPC results indicate that all three samples consist of pure PPO−PEO−PPO triblock co-polymers with the target molecular weight and chemical structure. Otherwise, the peaks for starting PEO in Scheme 1 with lower molecular weight might appear, or the polydisper-sities might be much broader as well as the unimodal peaks could not be achieved, if there were detectable impurities of unreacted PEO homopolymers and/or other species other than the target triblock copolymers. The $^1$H NMR spectra confirmed that the triblock copolymers consist of both PEO and PPO blocks. The ratios between the PEO and PPO block lengths could be determined from the integrals of peaks for PEO and PPO segments. In combination of the GPC with the $^1$H NMR results, the compositions and the PEO and PPO block lengths were calculated, which are also in good agreement with the elemental analysis results, as shown in Table 1.

It is important to ascertain that these triblock copolymers are terminated by PO segments. The $^{13}$C NMR spectroscopy has been used in the literature to identify the end-groups, and indicate whether a copolymer of EO and PO is a block or random copolymer.[16] Figure 1 shows the $^{13}$C NMR spectra of the PPO−PEO−PPO triblock copolymers as compared with the PEO and PPO homopolymers. In Figure 1a, the repetitive EO units of PEO give a single peak at 70.6 ppm. Variations in their

(14) The sonication as such was proved not to degrade either the copolymers or α-CD, by means of $^1$H NMR and GPC. Also see ref 8.
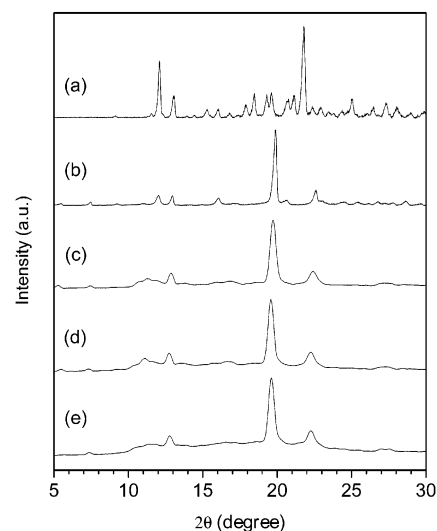
(15) (a) Zhou, Z.; Chu, B. *Macromolecules* **1994**, *27*, 2025−2033. (b) Mortensen, K.; Brown, W.; Jorgensen, E. *Macromolecules* **1994**, *27*, 5654−5666. (c) Mortensen, K. *Macromolecules* **1997**, *30*, 503−507.
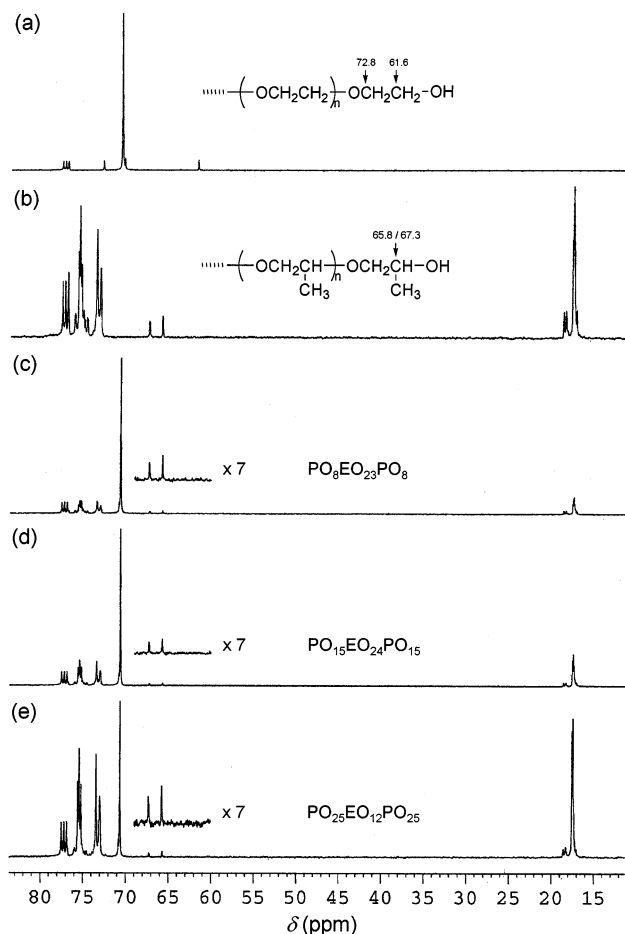
**Figure 1.** 100-MHz $^{13}$C NMR spectra for (a) PEO ($M_n$ 1000), (b) PPO ($M_n$ 1000), (c) $PO_8EO_{23}PO_8$, (d) $PO_{15}EO_{24}PO_{15}$, and (e) $PO_{25}EO_{12}PO_{25}$ in CDCl$_3$.



**Figure 2.** X-ray powder diffraction diagrams for the α-CD-propionic acid IC (a), α-CD-PEO ($M_n$ 1000) IC (b), α-CD-$PO_8EO_{23}PO_8$ polypseudorotaxane (c), α-CD-$PO_{15}EO_{24}PO_{15}$ polypseudorotaxane (d), and α-CD-$PO_{25}$-$EO_{12}PO_{25}$ polypseudorotaxane (e).

chemical shifts occur only near the ends of the PEO chain. The peaks at 61.6 and 72.8 ppm indicate the hydroxyl-bearing carbon and the ether carbon of the EO end-group, respectively.[16a] In Figure 1b, the peaks at 65.8 and 67.3 ppm indicate a terminal PO unit.[16b] In the spectra of the PPO−PEO−PPO triblock copolymers (Figure 1c, d and e), a strong singlet at 70.6 ppm suggests the presence of the PEO block. The peaks for the terminal PO unit clearly appear, whereas those for the EO end-group are not detected, suggesting that the PPO segments are located at the two ends of the PPO−PEO−PPO triblock copolymer, and there are no free terminals of PEO segments in the triblock copolymers.

When testing the IC formation between CDs and the PPO−PEO−PPO triblock copolymers, we found the copolymers formed ICs with α-CD as well as β- and γ-CD to give polypseudorotaxanes. The α-CD-PPO−PEO−PPO polypseudorotaxanes were formed in very high yields (71−83%), indicating that the IC formation was not due to any contamination of the copolymers. The formation of polypseudorotaxanes between α-CD and the PPO−PEO−PPO triblock copolymers is of special interest because a PPO chain was previously though to be impenetrable to the small cavity of α-CD. The α-CD-

PPO−PEO−PPO polypseudorotaxanes dissolved slowly when they were resuspended in a large amount of water, indicating that the IC formation is reversible, and the polypseudorotaxanes were in equilibrium in solution with their components.

Figure 2 shows the X-ray powder diffraction patterns of the α-CD-PPO−PEO−PPO polypseudorotaxanes and other α-CD ICs. In Figure 1a, the pattern of α-CD-propionic acid IC represents a cage-type structure of α-CD ICs.[17] In Figure 1b, the pattern of α-CD-PEO IC with a number of sharp reflections and the main one at $2\theta = 19.4°$ ($d = 4.57$ Å) represents the channel-type structure of crystalline necklace-like polypseudorotaxanes of α-CD and PEO,[12,17] which is totally different from that of α-CD-propionic acid IC. In the diagrams of the α-CD-PPO−PEO−PPO polypseudorotaxanes (Figure 2c, d, and e), the main parts of the patterns are similar to the diagram of the α-CD-PEO IC, suggesting that the α-CD-PPO−PEO−PPO polypseudorotaxanes are mainly composed of crystalline IC domains that are isomorphous with the channel-type structure formed by the α-CD-PEO IC.

Figure 3 shows the solid-state $^{13}$C CP/MAS NMR spectra of uncomplexed α-CD and the α-CD-$PO_{15}EO_{24}PO_{15}$ polypseudorotaxane. The α-CD molecule is known to assume a less symmetrical conformation in the crystalline uncomplexed state.[18] In this case, the spectrum shows resolved C-1 and C-4 resonances. Especially, resonances for C-1 and C-4 adjacent to a single conformationally strained glycosidic linkage are observed in the spectrum.[19] In contrast, the resolved resonances disappear in the spectra of α-CD-PPO−PEO−PPO polypseudorotaxanes, and each carbon of the glucose unit is observed as a single peak. The results indicate that the α-CD molecules in the polypseudorotaxanes adopt a symmetrical conformation, and each glucose unit of α-CD is in a similar environment,[8b] which further supports the IC formation between α-CD and the PPO−PEO−PPO triblock copolymers.

(16) (a) Barrelle, M.; Beguin, C.; Tessier, S. *Org. Magn. Reson.* **1982**, *19*, 102−104. (c) Schilling, F. C.; Tonelli, A. E. *Macromolecules* **1986**, *19*, 1337−1343. (b) Heatley, F.; Luo, Y. Z.; Ding, J. F.; Mobbs, R. H.; Booth, C. *Macromolecules* **1988**, *21*, 2713−2721. (d) Heatley, F.; Ding, J. F.; Yu, G. E.; Booth, C.; Blease, T. G. *Macromol. Chem., Rapid Commun.* **1993**, *14*, 819−823.

(17) (a) Takeo, K.; Kuge, T. *Agr. Biol. Chem.* **1970**, *34*, 1787−1794. (b) McMullan, R. K.; Saenger, W.; Fayos, J.; Mootz, D. *Carbohydr. Res.* **1973**, *31*, 37−46. (c) Atwood, J. L.; Davies, J. E. D.; MacNicol, D. D. *Inclusion Compounds,* Academic Press: New York, 1984.
(18) Manor, P. C.; Saenger, W. *J. Am. Chem. Soc.* **1974**, *96*, 3630−3639.
(19) Gidley, M. J.; Bociek, S. M. *J. Am. Chem. Soc.* **1988**, *110*, 3820−3829.
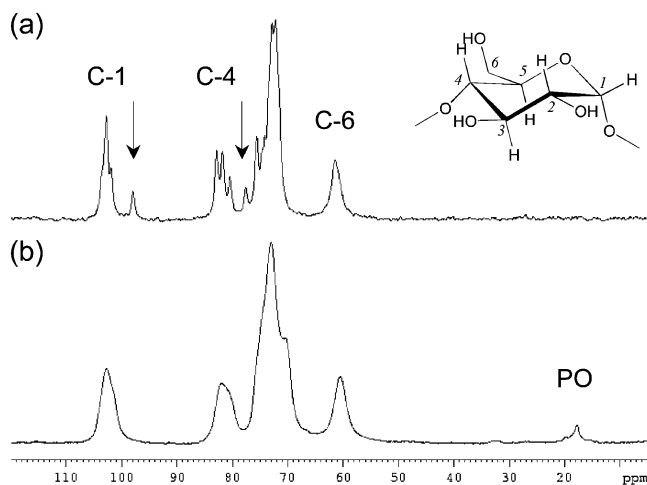
**Figure 3.** ^{13}C CP/MAS NMR spectra of uncomplexed α-CD (a) and α-CD-PO$_{15}$EO$_{24}$PO$_{15}$ polypseudorotaxane (b). The arrows show the resolved resonances for C-1 and C-4 adjacent to a single conformationally strained glycosidic linkage.
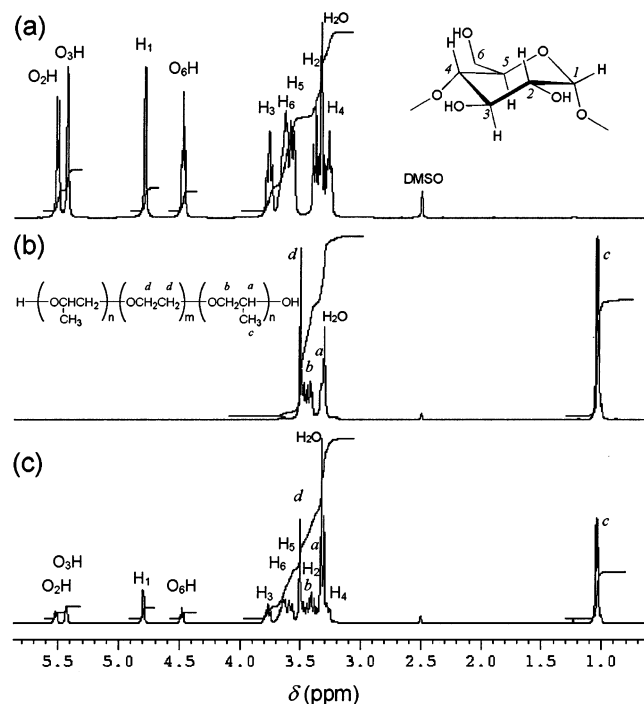


**Figure 4.** 400-MHz ^{1}H NMR spectra of α-CD (a), PO$_{25}$EO$_{12}$PO$_{25}$ (b), and α-CD−PO$_{25}$EO$_{12}$PO$_{25}$ polypseudorotaxane (c) in DMSO-$d_6$.

The compositions of the α-CD-PPO−PEO−PPO polypseudorotaxanes were quantitatively studied using ^{1}H NMR spectroscopy. Figure 4 shows the ^{1}H NMR spectrum of an α-CD-PPO−PEO−PPO polypseudorotaxane compared with its precursors. The copolymers in the polypseudorotaxanes were found to be identical to those before the formation of polypseudorotaxanes in terms of the molecular weights and block lengths. A comparison between the integral intensities of peaks for α-CD and those for PPO−PEO−PPO gives the compositions of the α-CD-PPO−PEO−PPO polypseudorotaxanes. The compositions determined from ^{1}H NMR spectroscopy were also found to be in good agreement with the elemental analysis results. Table 2 lists the numbers of α-CD in a single polypseudorotaxane chain (*x*). There are three possible structures for the α-CD-PPO−PEO−PPO polypseudorotaxanes: (a) the α-CD

**Table 2.** Composition and Stoichiometry of the α-CD-PPO−PEO−PPO Polypseudorotaxanes

| polypseudorotaxane | $x^a$ | $m/x^b$ | $2n/x^c$ | $(2n + m)/x^d$ |
|---|---|---|---|---|
| α-CD-PO$_8$EO$_{23}$PO$_8$ | 11.4 | 2.0 | 1.4 | 3.4 |
| α-CD-PO$_{15}$EO$_{24}$PO$_{15}$ | 11.4 | 2.1 | 2.6 | 4.7 |
| α-CD-PO$_{25}$EO$_{12}$PO$_{25}$ | 5.6 | 2.1 | 8.9 | 11.1 |

[a] The number of α-CD in a single polypseudorotaxane chain determined by ^{1}H NMR. [b] Molar ratio of EO unit to α-CD. [c] Molar ratio of PO unit to α-CD. [d] Molar ratio of total number of EO and PO units to α-CD.

molecules are selectively threaded on the middle PEO block, whereas the PPO blocks remain uncovered; (b) the α-CD molecules are selectively threaded on the flanking PPO blocks, whereas the middle PEO block remains uncomplexed; and (c) the α-CD molecules are threaded on both PEO and PPO blocks. As shown in Table 2, the molar ratio of EO unit to α-CD (*m/ x*), corresponding to the assumption of a), is 2:1 for all three polypseudorotaxanes, which matches perfectly the stoichiometry of the α-CD-PEO ICs reported previously.[8b] This strongly suggests that in the α-CD-PPO−PEO−PPO polypseudorotaxanes, only the middle PEO block is closely included by α-CD molecules, whereas the flanking PPO blocks are uncovered. In contrast, the molar ratios of PO unit to α-CD (2n/x) or total number of PO and EO units to α-CD [(2*n* + *m*)/*x*], corresponding to the assumptions of (b) or (c), show no consistency with any reasonable schoichiometry at all.

On the basis of these findings we can reasonably hypothesize that the IC formation is driven by the strong interaction between α-CD and the PEO segments, and aided by the flexible molecular motion of α-CD and the copolymer chain. The proposed structure is also in accordance with the broadening X-ray powder patterns for the α-CD-PPO−PEO−PPO polypseudorotaxanes (Figure 2c, d, and e), which show that the polypseudorotaxanes have a lower crystallinity than the stoichiometric α-CD-PEO ICs, most likely caused by the existence of the uncovered amorphous PPO blocks. Mayer et al.[20] have performed computational studies on the IC formation between α- or β-CD and oligomers of PEO, PPO, or PEO−PPO diblock copolymer up to EO$_4$PO$_4$. Their simulation estimates a total complexation energy of −52.4 kJ/mol for α-CD-PEO compared with −43.3 kJ/mol for α-CD-PPO, supporting our hypothesis that there is incentive for α-CD to overcome an energy barrier to reach the middle PEO block.
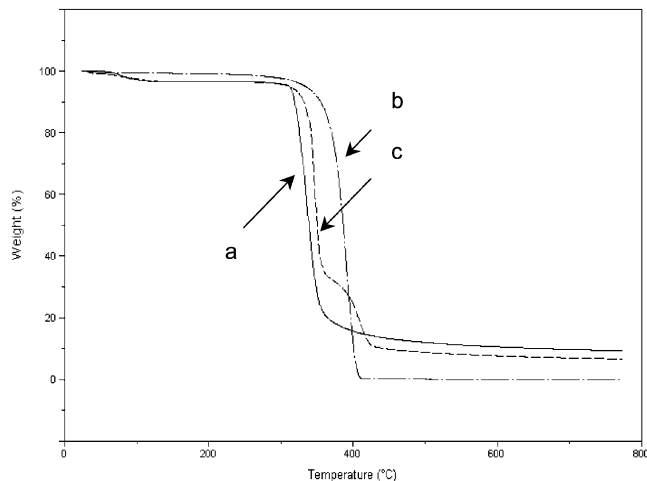
Differential scanning calorimetry (DSC) was carried out to get the information on glass transition temperatures ($T_g$) for the PO segments in the free copolymers and the polypseudorotaxanes. Figure 5 shows the DSC thermograms for all three PPO−PEO−PPO triblock copolymers and their polypseudorotaxanes formed with α-CD. The DSC thermogram for pure α-CD is also presented in Figure 5 for comparison. As shown in Figure 5a, all three triblock copolymers have clear glass transitions for the PPO blocks at a narrow temperature range from −64 to −69 °C. The $T_g$ values of PO$_8$EO$_{23}$PO$_8$ (−64 °C) and PO$_{15}$-EO$_{24}$PO$_{15}$ (−66 °C) are slightly higher than that of PO$_{25}$EO$_{12}$-PO$_{25}$ (−69 °C), because the first two have longer PEO blocks that form crystalline phases, which restrict the molecular motion of PPO blocks to some extent. As shown in Figure 5b, α-CD does not show any thermal transitions during the course of heating. It should be noted that stoichiometric α-CD-PEO and

(20) Mayer, B.; Klein, C. T.; Topchieva, I. N.; Kohler, G. *J. Comput.-Aided Mol. Des.* **1999**, *13*, 373−383.
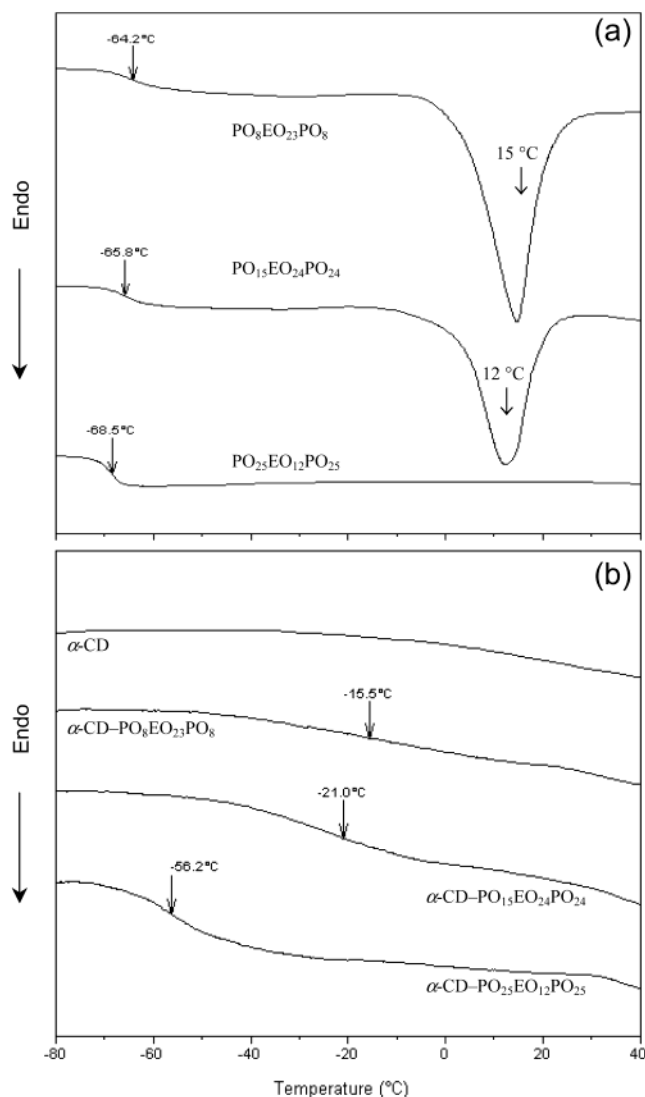
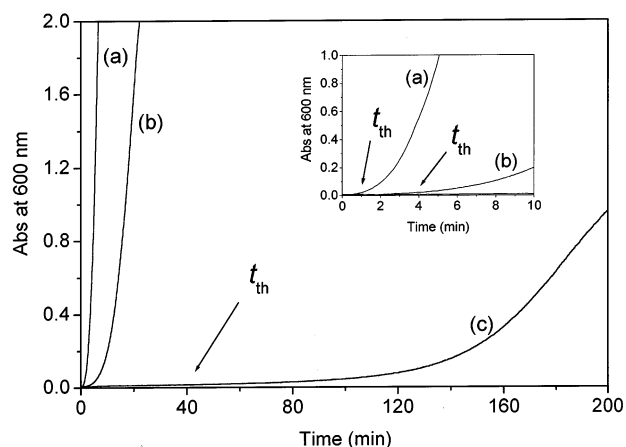**Figure 5.** DSC thermograms (second heating run at 20 °C/min) for: (a) the PPO−PEO−PPO triblock copolymers; (b) α-CD and the α-CD-PPO−PEO−PPO polypseudorotaxanes.



**Figure 6.** TGA curves obtained at a heating rate of 20 °C/min under nitrogen atmosphere for (a) α-CD, (b) $PO_{15}EO_{24}PO_{15}$, and (c) α-CD−$PO_{15}$-$EO_{24}PO_{15}$ polypseudorotaxane.



**Figure 7.** Plot of absorbance as a function of time for aqueous solutions containing 126 mg/mL of α-CD and 6.5 mg/mL of triblock copolymer $PO_8$-$EO_{23}PO_8$ (a), $PO_{15}EO_{24}PO_{15}$ (b), and $PO_{25}EO_{12}PO_{25}$ (c) at 20 °C. The arrows indicate the region where absorbance remains zero. The inset shows an expanded plot for 0 to 10 min.

β-CD-PPO ICs studied previously also present no thermal transitions before decomposition because every single polymer chain is closely included in the channels formed by CDs in those ICs. In Figure 5b, α-CD-$PO_8EO_{23}PO_8$, α-CD-$PO_{15}EO_{24}PO_{24}$, and α-CD-$PO_{25}EO_{12}PO_{25}$ polypseudorotaxanes present glass transitions for the PO segments at −16, −21, and −56 °C, respectively, indicating that the PPO blocks in the polypseudorotaxanes are uncovered by α-CD and remain amorphous, which agrees with our hypothesis that only PEO block is closely covered by α-CD in these polypseudorotaxanes. It is notable that the $T_g$ values of the PPO−PEO−PPO triblock copolymers in the polypseudorotaxanes significantly increases by 49, 45, and 12 °C, respectively, as compared with their free copolymer counterparts. This may be caused by the rigid crystalline phases of the IC domains formed by α-CD and the middle PEO block, which strongly confine the PPO blocks in the polypseudorotaxanes. The increases in $T_g$ values for α-CD-$PO_8EO_{23}PO_8$ and α-CD-$PO_{15}EO_{24}PO_{24}$ polypseudorotaxanes are more significant than α-CD-$PO_{25}EO_{12}PO_{25}$ polypseudorotaxane because the first two have larger IC domains formed by the longer PEO blocks,

as well as the higher weight ratios of the IC to the amorphous PPO domains.

The thermal stability of the α-CD-PPO−PEO−PPO polypseudorotaxanes was evaluated using thermogravimetric analysis (TGA) and compared with free α-CD and the starting triblock copolymers. Figure 6 shows the weight loss curves for α-CD-$PO_{15}EO_{24}PO_{15}$ polypseudorotaxane and its precursors. The polypseudorotaxane undergoes two-step thermal degradation. The first step can be mainly attributed to decomposition of α-CD, while the second one mainly to $PO_{15}EO_{24}PO_{15}$ copolymer. Although the polypseudorotaxane and free α-CD start to decompose at similar temperatures ranging from 293 to 300 °C, the course of weight loss for the complexed α-CD is obviously slower than free α-CD. We use the temperature at which 10% of mass loss has occurred after a certain component starting decomposition as the decomposition temperature ($T_d$) to quantitatively evaluate the thermal stability,[21] and the results for all three polypseudorotaxanes are listed in Table 3. The $T_d$ values for α-CD in the polypseudorotaxanes increased by 8−11

(21) Arnal, M. L.; Balsamo, V.; Lopez-Carrasquero, F.; Contreras, J.; Carrillo, M.; Schmalz, H.; Abetz, V.; Laredo, E.; Muller, A. J. *Macromolecules* **2001**, *34*, 7973−7982.

***Table 3.*** Decomposition Temperatures[a] ($T_d$) of the α-CD-PPO−PEO−PPO Polypseudorotaxanes in Comparison with Their Free Components, and the α-CD Contents in the Polypseudorotaxanes Estimated from ^{1}H NMR and TGA

| | $T_{d \text{ (free)}}$[b] (°C) | | $T_{d \text{ (PPR)}}$[c] (°C) | | α-CD content (wt %) | |
|---|---|---|---|---|---|---|
| polypseudorotaxane | α-CD | PPO–PEO–PPO | α-CD | PPO–PEO–PPO | ^{1}H NMR | TGA |
| α-CD-PO$_8$EO$_{23}$PO$_8$ | 321 | 364 | 329 (+8) | 382 (+18) | 85 | 81 |
| α-CD-PO$_{15}$EO$_{24}$PO$_{15}$ | 321 | 358 | 332 (+11) | 386 (+28) | 80 | 73 |
| α-CD-PO$_{25}$EO$_{12}$PO$_{25}$ | 321 | 360 | 332 (+11) | 383 (+23) | 61 | 57 |

[a] Temperatures at which 10% of mass loss has occurred from TGA curves. [b] $T_d$ for free α-CD and free PPO−PEO−PPO triblock copolymers. [c] $T_d$ for each component in the polypseudorotaxanes. The numbers in the brackets indicate the increases of $T_d$ for each component in the polypseudorotaxanes as compared with their free counterparts.
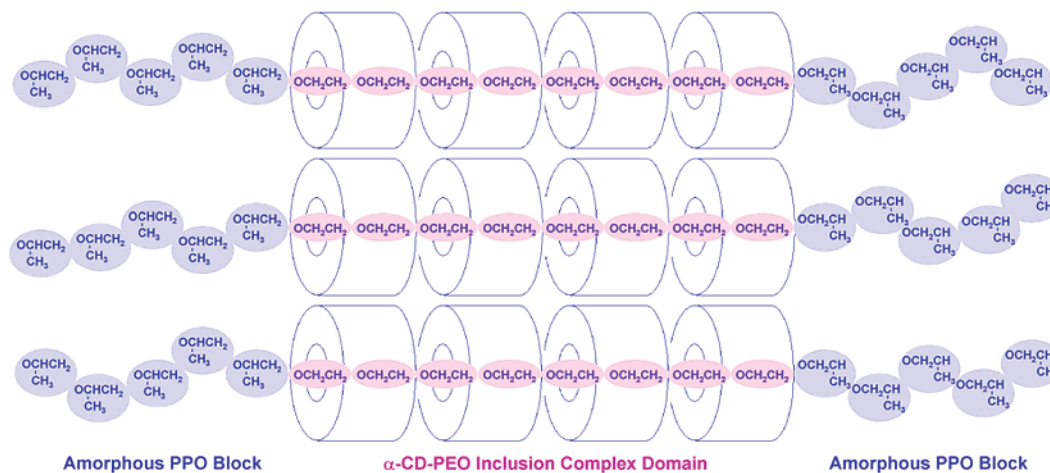


***Figure 8.*** Schematic representation of the proposed structure of the α-CD−PPO−PEO−PPO polypseudorotaxanes, where the thinner middle PEO blocks form inclusion complex domains with α-CD, whereas the flaking thicker PPO blocks are uncomplexed and remain amorphous.

°C, and those for the copolymers in the polypseudorotaxanes increased by 18−28 °C, as compared with their respective free counterparts. Therefore, both α-CD and the triblock copolymers were stabilized by formation of the polypseudorotaxanes. In addition, the two-step weight loss behavior can be used to estimate the ratio between α-CD and the copolymers in the polypseudorotaxanes. Although the TGA method may not be as accurate as the ^{1}H NMR due to the partially overlapping of the two weight loss steps, the α-CD contents estimated from TGA results are in quite good agreement with those determined by ^{1}H NMR spectroscopy, as shown in Table 3.

The kinetics of the threading process and formation of the ICs were studied with turbidity measurements. Figure 7 shows the absorption change during formation and precipitation of the polypseudorotaxanes between α-CD and PPO−PEO−PPO triblock copolymers in aqueous solution. The curves show a region where the absorption remains zero, followed by a region where the absorption sharply increases. The first region corresponds to the threading and sliding of α-CD onto the polymer chains, so the time for this region is defined as "threading time" ($t_{th}$).[9c] After $t_{th}$ stable polypseudorotaxanes are formed and they start to aggregate into crystalline particles. Therefore, the absorption starts to increase sharply in the second region. Figure 7 shows that the $t_{th}$ increases from ca. 1.0 min for PO$_8$EO$_{23}$PO$_8$ ($n = 8$), to ca. 4.0 min for PO$_{15}$EO$_{24}$PO$_{15}$ ($n = 15$) and ca. 40 min for PO$_{25}$EO$_{12}$PO$_{25}$ ($n = 25$). The $t_{th}$ is strongly dependent on the length of the PPO blocks, because the α-CD molecules have to first overcome the energy barrier, threading and sliding over the flanking PPO blocks, before forming stable IC with the middle PEO block.

## Conclusions

A series of new polypseudorotaxanes were synthesized in high yields when the middle PEO block of PPO−PEO−PPO triblock copolymers was selectively recognized and included by α-CD to form crystalline ICs. X-ray diffraction and solid-state CP/MAS ^{13}C NMR studies showed that the IC domains of the polypseudorotaxanes assume channel-type structure, and the α-CD molecules in the polypseudorotaxanes adopt a symmetrical conformation due to formation of the ICs. The DSC analysis showed that the PPO blocks in the polypseudorotaxanes are uncovered by α-CD and remain amorphous. The TGA results revealed that the polypseudorotaxanes have better thermal stability than their free components due to the inclusion complexation. The compositions and stoichiometry of the polypseudorotaxanes were determined from ^{1}H NMR and TGA results, and a 2:1 (EO unit to α-CD) stoichiometry was found for all polypseudorotaxanes, although the PPO−PEO−PPO triblock copolymers have different compositions and block lengths, suggesting that only the PEO blocks are closely included by α-CD molecules. Finally, the kinetic studies of the threading process of α-CD onto the copolymers revealed that the threading time is strongly dependent on the PPO block lengths, because the α-CD molecules have to first overcome the energy barrier to slide over the flanking PPO blocks, before forming stable ICs with the middle PEO block. On the basis of our results, a schematic illustration of the structure of the α-CD-PPO−PEO−PPO polypseudorotaxanes is presented in Figure 8.

The unexpected findings reported in this article contradict the conventional wisdom that α-CD would not be large enough to slide over a PPO chain. In the meantime, we also found an important fact that the α-CD molecules would not "stick" on

the PPO blocks while they slide over the PPO blocks toward the middle PEO block, because of the unfavorable complexation energy for α-CD and PPO segments. This well explains why a PPO homopolymer could not form an IC with α-CD. This report may represent an important contribution to the understanding of the mechanism involved in the IC formation between polymers and cyclodextrins, while the findings may have intriguing implications in designing new cyclodextrin ICs and polypseudorotaxanes using novel functional block copolymers, for molecular machines, sensors, or other interesting applications.

**Supporting Information Available:** GPC and ^{1}H NMR data for the PPO−PEO−PPO triblock copolymers. This material is available free of charge via the internet at http://www.pubs.acs.org.

JA026623P